

**DEVELOPMENT OF A MULTIWAVELENGTH
AIRBORNE POLARIMETRIC LIDAR FOR
VEGETATION REMOTE SENSING**

By

Songxin Tan

A DISSERTATION

Presented to the Faculty of
The Graduate College at the University of Nebraska
In Partial Fulfillment of Requirements
For the Degree of Doctor of Philosophy

Major: Interdepartmental Area of Engineering
(Electrical Engineering)

Under the Supervision of Professor Ram M. Narayanan

Lincoln, Nebraska

August, 2003

UMI Number: 3102576

UMI[®]

UMI Microform 3102576

Copyright 2003 by ProQuest Information and Learning Company.
All rights reserved. This microform edition is protected against
unauthorized copying under Title 17, United States Code.

ProQuest Information and Learning Company
300 North Zeeb Road
P.O. Box 1346
Ann Arbor, MI 48106-1346

DISSERTATION TITLE

Development of a Multiwavelength Airborne Polarimetric

Lidar for Vegetation Remote Sensing

BY

Songxin Tan

SUPERVISORY COMMITTEE:

Approved

Date

Ram M. Narayanan

8/4/03

Signature

Ram M. Narayanan

Typed Name

Dennis R. Alexander

8/04/03

Signature

Dennis R. Alexander

Typed Name

John A. Woollam

8/4/03

Signature

John A. Woollam

Typed Name

Donald C. Rundquist

8/4/03

Signature

Donald C. Rundquist

Typed Name

Signature

Typed Name

Signature

Typed Name

Nebraska UNIVERSITY OF GRADUATE COLLEGE

DEVELOPMENT OF A MULTIWAVELENGTH AIRBORNE POLARIMETRIC LIDAR FOR VEGETATION REMOTE SENSING

Songxin Tan, Ph.D.

University of Nebraska, 2003

Advisor: Ram M. Narayanan

A Multiwavelength Airborne Polarimetric Lidar (MAPL) system has been developed for vegetation remote sensing purposes to support the Airborne Remote Sensing Program at the University of Nebraska. The MAPL design and instrumentation are described in detail. Characteristics of the MAPL system include dual-wavelength detection, lidar waveform capture, and polarimetric measurement, which provide enhanced opportunities for vegetation remote sensing, compared to current sensors. Vegetation canopy models, for a single tree and for the three dimensional forests, are developed for airborne lidar applications; and efforts are made towards modeling the vegetation lidar waveform. This study also develops the theoretical analysis for the vegetation canopy lidar, by combining the lidar equation with the canopy models. The noise sources that may affect the performance of the MAPL are discussed and the ground signal to noise ratio (SNR) under the vegetation cover conditions is also investigated. The optical alignment of the MAPL system is briefly introduced. Polarimetric calibration of the system by laboratory measurements of the Stokes parameters of various materials is discussed. Range detection ability was field tested and calibrated. To validate the system's ability for vegetation canopy detection, extended ground tests were performed on the separate trees and the forest detection. Efforts were also made toward a tree species discrimination algorithm applying the MAPL data. Backscattered polarimetric returns, the depolarization ratios, polarimetric normalized difference vegetation indices, and polarimetric band ratios are presented in this dissertation; many of them are obtained for the first time.

Acknowledgments

The author would like to express his appreciations to the following professors for their inspiration, encouragement, support, and assistance. First, I would like to express my immense gratitude to my academic advisor, Professor Ram M. Narayanan, for offering me this research opportunity to work on airborne lidar and being an excellent mentor. His great academic management style is highly appreciated. I would like to thank Professor Dennis R. Alexander, for providing logistic support, serving on my committee, and making himself available for helps and discussions. Special thanks are due to Professor Donald C. Rundquist and Professor John A. Woollam, for volunteering to be on my committee, and for many helpful comments and suggestions during my study and preparation of this dissertation.

The Multiwavelength Airborne Polarimetric Lidar (MAPL) project is a very challenging project. It would be impossible to complete the lidar sensor without various assistances and supports from many organizations and individuals. The author would like to thank NASA Goddard Space Flight Center (GSFC) for providing the ALPS instrument, part of which was used in developing the MAPL system. Special thanks are due to Dr. James E. Kalshoven of NASA GSFC, for his constant technical support during the design and construction of the MAPL system. Thanks are also due to Dr. Steve Vanstone of Redstone Arsenal, Alabama, for providing information on modification of the ALPS. The author would like to thank Professor Mangzuo Shen of the Institute of Optics and Electronics, Chinese Academy of Sciences, Chengdu, China, for his many helps at the initial phase of this project, especially in optical installation and alignment. Special thanks to Dr. James Churnside and Dr. Jim Wilson of the Environmental Technology Laboratory at NOAA for sharing information on the Fish Lidar and laser safety. The author would like to extend his thanks to the members of the Center for Advanced Land Management Information Technologies (CALMIT) at the University of Nebraska, for their

constant assistances in field test and aircraft installation of the MAPL. Mr. Kelvin Seevers and Rick Perk provided help on aircraft installation; Mr. Bryan Leavitt provided spectral reflectance measurement of a canvas tarp; and Mr. Jeff Moon helped in searching field test sites. Many thanks to Dr. Mike Larson and pilot Brian Bronson at the Aviation institute of the University of Nebraska at Omaha, for providing support on aircraft installation. Thanks to Ms. Karen Schurr of the Department of Civil Engineering for providing a range measurement standard, and to Professor James Brandle at the School of Natural Resources for providing help on forest descriptions. The members (including many former members) of the Environmental Remote Sensing Laboratory (ERSL) at the University of Nebraska provided numerous helps during the years. In particular, I would like to send my appreciation and thanks to Professor Robert D. Palmer, Dr. Mohammad Dawood, Dr. Xiaojian Xu, Brian Corner, Wei Zhou, Yeqing Huang, Guangdong Pan, Yan Zhang, Paul Cantu, Cihan Kumru and many others.

Last but not least, I owe a debt of gratitude to my family. I would like to thank my great parents for their endless love, constant support, and unwavering faith in me even in face of adversities and setbacks. Special thanks to my dear wife, Zixing, for her ever-presenting love, constant encouragement, emotional comfort, and her confidence in me. Through her love and support, she makes my vision of future clearer and my life more enjoyable.

Table of Contents

Acknowledgments	i
Table of Contents	iii
List of Figures	vi
List of Tables	ix
1. Introduction and Background	1
1.1 Introduction to Lidar	1
1.2 Airborne Vegetation Laser Sensors	3
1.3 Lidar Vegetation Remote Sensing	6
1.3.1 Importance of Vegetation Canopy Remote Sensing	6
1.3.2 Advantages of Vegetation Lidar	7
1.3.3 Vegetation Vertical Structure Detection	8
1.3.4 Lidar Polarimetric Measurement	10
1.4 Motivation for a New Lidar Sensor	10
1.5 Organizational Overview	11
2. MAPL System Description	12
2.1 System Introduction	12
2.2 Nd:YAG Laser Source	15
2.3 Receiving Optics	17
2.4 Data Acquisition and Processing	19
2.5 Airborne Specifications	19
3. Theoretical Foundation of Lidar	21
3.1 Lidar Range Equation	21
3.2 Atmospheric Transmittance and Depolarization	24
3.3 Lidar Return Energy under Various Conditions	27

3.4	Photomultiplier Tube as Photodetector	30
3.5	Signal to Noise Ratio (SNR) Analysis	31
3.5.1	Quantum Noise	32
3.5.2	Background Noise	33
3.5.3	Dark Current noise	34
3.5.4	Thermal Noise	35
3.5.5	System Signal to Noise Ratio (SNR)	36
3.5.6	Noise Reduction Techniques	37
3.6	Laser Safety Considerations	39
4.	Lidar Canopy Models	44
4.1	Background	44
4.2	A Canopy Vertical Distribution Model	45
4.3	3-D Vegetation Models	52
4.3.1	Stand Distribution	53
4.3.2	Non-overlapping 3-D model	57
4.3.3	Overlapping 3-D Model	64
4.4	Vegetation Lidar Equation	70
4.5	Ground SNR under Vegetation Cover	70
5.	MAPL System Alignment	73
5.1	Introduction	73
5.2	Receiving Optics Alignment	74
5.3	Laser Beams and Receivers Alignment	76
6.	Polarimetric Calibration Efforts	78
6.1	Modification of the ALPS	78
6.1.1	Laser Source	82
6.1.2	Polarization Receiving Optics	82

6.2	Laboratory Experimental Setup	84
6.3	Stokes Parameters Measurement	85
6.4	Experimental Results	90
6.5	Polarimetric Calibration Procedure	96
7.	Range Measurement and Calibration	98
7.1	Principle of Range Detection	98
7.2	Range Calibration	99
7.3	Small Target Detection	104
8.	Applications in Ground Tree Detection	106
8.1	Separate Trees	106
8.2	Forest	110
8.3	Tree Species Discrimination	119
8.4	Other Applications	123
9.	Conclusions and Future Research Directions	126
9.1	Conclusions and Contributions	126
9.2	Future Research Directions	128
9.2.1	Lidar Instrumentation	128
9.2.2	Lidar Vegetation Model	130
9.2.3	Polarimetric Calibration	131
9.2.4	New Applications	132
	References	133
	Appendix A Laser Hazard Evaluations	142
	Appendix B Schematic Layout of MAPL Aircraft Installation	146
	Appendix C Lidar Installation Design Drawings	147

List of Figures

1.1 A typical lidar system.	2
2.1 The MAPL system block diagram.	12
2.2 (a). Bottom view of the lidar assembly.	13
2.2 (b). Front view of the lidar assembly.	14
2.2 (c). Rack mount of the electronics devices.	14
2.3 The MAPL receiving optics configuration.	18
2.4 The MAPL laser footprint pattern.	20
3.1 Illustration of a Lambertian reflection surface.	23
3.2 One way atmospheric transmittance at 1064-nm and 532-nm.	26
3.3 Lidar return at different range and transmitted energy levels.	29
3.4 Lidar return energy changes as receiver aperture diameter changes.	29
3.5 Lidar received energy at dual wavelength and dual polarization from a bare ground. ..	30
3.6 A typical temperature characteristic curve of dark current.	35
3.7 System SNR at dual-polarization and dual-wavelength from a bare ground.	37
3.8 Radiant exposure for 1064 nm at 63 mJ output level.	42
3.9 Radiant exposure from 532 nm at 36 mJ output level.	43
4.1 A typical airborne lidar vegetation remote sensing scenario.	47
4.2 Three simulated canopy shapes.	49
4.3 The foliage area density profiles.	50
4.4 The penetration functions.	50
4.5 The relative lidar waveforms.	52
4.6 The probability distribution functions of Poisson, Neyman Type A, and discrete uniform process, where $m = 50$, $m_1 = 10$, $m_2 = 5$, $n_1 = 15$, and $n_2 = 85$	56
4.7 A stand distribution of non-overlapping trees.	58
4.8 A 3-D sparse forest scene.	59
4.9 FWHM laser beamwidth.	60
4.10 Normalized lidar waveform from a non-overlapping forest at nadir angle.	62
4.11 Normalized lidar waveform from a non-overlapping forest at a slightly off-Nadir angle (5 degrees).	62
4.12 Comparison of the nadir and off-nadir lidar waveforms.	63

4.13 Normalized lidar waveforms from different sparse forest configurations.	64
4.14 Overlapping distribution of trees.	65
4.15 An overlapping tree stand distribution.	68
4.16 An overlapping 3-D forest scene.	69
4.17 Overlapping forest lidar waveform for nadir-looking case.	69
4.18 Comparison of the nadir and off-nadir (5 degrees) lidar waveforms.	70
4.19 Ground SNR under a dense forest condition.	71
4.20 Ground SNR under a 100% vegetation coverage condition.	72
5.1 Misalignment of the laser beam and detector FOV.	74
5.2 Optical configuration for receiving optics alignment.	75
5.3 Image of the detector field stops at a distance of 10 meters.	76
5.4 Field alignment of the MAPL system.	77
6.1 Receiver configuration of the old system. The laser beam is focused onto the PMT, causing non-uniform response.	80
6.2 Light distribution at the detector plane of the old system.	80
6.3 Modified receiving optics. The PMT receiving plane is uniformly illuminated.	81
6.4 Light distribution at the detector plane after modification.	81
6.5 Configuration of the polarization measurement elements.	83
6.6 Configuration of the four-channel Stokes parameters measurement.	84
6.7 Setup of the laboratory measurement.	85
6.8 A polarization ellipse.	86
6.9 Polarization ellipse change with phase difference $\Delta\epsilon$	87
6.10 Stokes parameters of backscattered laser light from different materials.	92
6.11 Depolarization, degree of polarization and ellipse angle of the backscattered light from different materials.	93
6.12 Laboratory measurement of the polarimetric reflectance of a canvas using modified ALPS system at 1064 nm and 532 nm.	95
6.13 Laboratory measurement of the polarimetric reflectance of a concrete using modified ALPS system at 1064 nm and 532 nm.	95
6.14 Canvas tarp non-polarimetric reflectance.	96
6.15 The Labview program for the MAPL calibration.	97
7.1 Timing diagram of laser Q-switch and output.	98

7.2 The MAPL system timing diagram.	99
7.3 Setup of a range measurement standard.	100
7.4 The repeated lidar returns from a wall target using MAPL system.	101
7.5 The repeated range measurement results from the four channels.	102
7.6 Measurement of the distance between two close targets.	103
7.7 Repeated measurement results of a small target.	104
7.8 A single returned waveform from the small target.	105
7.9 After averaging of 200 measurements, the small target is clearly seen at the range of 608.1 m.	105
8.1 Lidar ground test site.	107
8.2 Range–intensity image of the lidar return at different channels from the above scene..	107
8.3 Plot of the MAPL returns from Ch1 through Ch4.	108
8.4 Depolarization from IR and GN wavelengths.	108
8.5 One scan line of the lidar return.	109
8.6 Variation of the laser output energy.	110
8.7 The forest scene.	111
8.8 Color-coded image of the scanning data from the forest on May 14, 2002.	112
8.9 Polarimetric profile of forest.	113
8.10 Sample lidar waveforms from canopy scan data.	113
8.11 Forest depolarization data.	114
8.12 Polarimetric NDVI matrix of the forest.	116
8.13 Polarimetric band ratioing matrix of the forest.	117
8.14 Color-coded image of scanning data from the forest on May 20, 2002.	118
8.15 Different tree species and their corresponding lidar return signals.	120
8.16 Cloud lidar image on June 10, 2003.	125
9.1 Optical receiver configuration of a fully polarimetric imaging lidar.	130

List of Tables

1.1 Lidar categorized by footprint size.	4
2.1 Parameters of the Nd:YAG laser source.	16
2.2 Specifications of the MAPL receiving optics.	18
3.1 Atmosphere extinction coefficient and transmittance at 532 nm and 1064 nm.	26
3.2 Parameters for the lidar return energy computation.	28
3.3 Parameters of the PMT detectors.	31
4.1 Parameters for a sparse forest simulation.	59
6.1 Specifications of the Nd:YAG system for laboratory measurement.	82
6.2 Specifications of the receiving optics for laboratory measurement.	83
7.1 MAPL range measurement results compared with the results from the Sokkia SET600 electronic total station.	102
7.2 Measurement results of the distance between two close targets.	103
8.1 Average depolarization and percent reflectance of the trees.	122
8.2 Weather conditions (data obtained from US National Weather Service).	124

PREVIEW

Chapter 1

Introduction and Background

LIDAR is an acronym for Light Detection And Ranging. It is also called optical radar, laser radar or ladar [1] under different applications. The principle of lidar is similar to that of the microwave radar. However, lidar operates in the optical frequency region while radar works in the microwave frequency region. Since there are many unique mechanisms of light interaction with media, lidar differs in many respects from radar.

The idea of using a light source instead of a microwave source to probe the target actually came earlier than the first appearance of the laser. However, a laser is able to provide a light beam with high intensity, high collimation, high coherence, high spectral purity, and high polarization purity, and is therefore superior to any conventional light sources in these respects. For such reasons, all modern lidar systems use a laser as the radiation source.

1.1 Introduction to Lidar

A typical lidar system is composed of a laser source, transmitting optics, receiving optics, photodetector, analog-to-digital (A/D) converter, signal and data processor and output device. Fig. 1.1 shows the block diagram of a typical lidar system. The sequence of system operation is as follows. The laser beam is sent out through the transmitter towards the target, the transmitted light interacts with the media and is reflected/scattered back towards the receiving optics, the photodetector then turns the received light signal into an analog electrical signal, which is further transformed into a digital signal by an analog-to-digital (A/D) converter, the signal is analyzed by the signal and data processor, and the final results are sent to an output device. Lidar systems can be used to characterize a wide variety of targets, from a hard target such as a vehicle or a tree, to a pure phase object such as the atmosphere or the cloud. There exist various types of interactions

between light and media, which is detectable by a lidar. These interactions have different physical mechanisms, including Rayleigh scattering, Mie scattering, Raman scattering, resonance scattering, fluorescence, absorption, and differential absorption and scattering [2].

The development of lidar is strongly dependent on the technological advances in laser, photodetector, data sampling and data processing. From a pure technological point of view, however, the laser and the photodetector are two main bottlenecks limiting the application of lidar towards vegetation remote sensing. Laser systems are required to be more compact, more rugged and wavelength tunable. The ideal laser system requires good beam quality, high energy efficiency, high energy output, high stability, high pulse repetition rate, and short pulse duration. On the other hand, the photodetector is desired to have broad spectral response, high responsivity, high quantum efficiency, low dark current, and low noise. Photodetector arrays can be used to make scanless imaging lidar [3]. For many applications, high quantum efficiency, low-noise, and uncooled infrared detector array is in great demand.

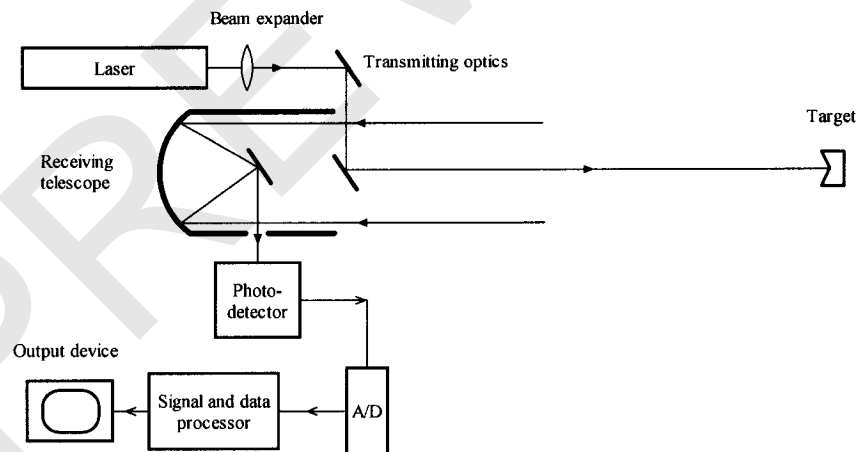


Figure 1.1 A typical lidar system.

Lidar can be categorized into different types through their functions, operating platforms, light and media interaction mechanisms, modulation and demodulation techniques, etc. For

example, based on detection schemes, they are grouped into direct detection lidar, coherent lidar and differential absorption lidar (DIAL); based on the laser source characteristics, they are grouped into continuous wave (CW) lidar and pulse lidar; and based on the transmitter and receiver configurations, they are grouped into monostatic and bistatic lidar.

Lidar is used to detect target distance, speed, rotation and vibration, similar to traditional radar. It is also applied for chemical composition and concentration studies [4] using DIAL technology. The various applications of lidar include rangefinder, altimetry, velocimetry, bathymetry, vibration sensor, moving target indicator (MTI), target detection and identification, aerosol detection, chemical and biological agent detection, among many others.

Because of the many unique characteristics of laser beam, it is natural to apply lidar in a wide variety of remote sensing applications. Since its first appearance in the 1960s, lidar has become an important active optical remote sensing tool. Lidar systems have found wide applications in such remote sensing areas as atmospheric remote sensing [5], oceanographic remote sensing [6], space remote sensing [7], hydrologic remote sensing [8], geographic remote sensing [9], and vegetation remote sensing [10]-[30], etc.

1.2 Airborne Vegetation Laser Sensors

Airborne vegetation lidar is still a new technology in many respects. The early lidar system used in vegetation remote sensing was a laser altimeter, which originally refers to a laser sensor used to detect either the first or the last laser return for altitude measurement. Due to the detector and A/D converter limitations, it is unable to digitize the whole laser return signal, or the so-called lidar waveform. In vegetation remote sensing, the recorded laser return signal as a function of time or range is often referred to as the lidar waveform [31]. The laser altimeter can only sample one point at a time. However, there is a trend among the remote sensing community to call lidar capable of entire waveform digitization as a laser altimeter. Most early vegetation lidar systems

have a small footprint, typically less than 1 m. Recent research found that small footprint lidar tends to underestimate the vegetation height, because the laser beam may frequently miss the canopy tops [16], [20], [22], [26]. Increasing the lidar footprint, which sacrifices the spatial resolution, improves the ability of lidar in forest remote sensing. More lidar systems with medium to large footprints are designed [14]. Table 1.1 lists the typical footprint sizes for lidar systems. One exception is to use the high pulse repetition frequency (PRF) laser scanner. Even though the footprint of such a laser scanner is usually very small, it is still possible to locate each individual tree, and estimate the single stand forest attributes [21], as a result of the high frequency.

Table 1.1 Lidar categorized by footprint size.

Small footprint	≤ 1 m
Medium footprint	1 – 10 m
Large footprint	≥ 10 m

Listed below are several airborne laser sensors designed specifically for vegetation remote sensing purpose.

ALPS: The Airborne Laser Polarimetric Sensor (ALPS) system, developed by NASA Goddard Space Flight Center (GSFC), is a laser polarimeter used for vegetation remote sensing [32]. It is the first multispectral laser polarimeter. The ALPS system employs a linearly polarized laser source at both 1064 nm and 532 nm. The laser pulse width is 7 ns, pulse repetition rate is 0.5 Hz and pulse energy is 30 mJ at each wavelength. Twelve photo multiplier tube (PMT) detectors are adopted in the system, providing the Stokes parameters measurement ability. The detector FOV is about 0.03 radians. The data acquisition system uses a Kenetic CAMAC system, with a 12-channel LeCroy 2249W analog-to-digital (A/D) converter. The platform is a helicopter, hovering typically below 300 m altitude. ALPS cannot acquire the lidar waveform.

SLICER: The Scanning Lidar Imager of Canopy by Echo Recovery (SLICER) is a large

footprint, high altitude, airborne system that can digitize the entire lidar waveform, developed by NASA GSFC [33]. The SLICER employs a Nd:YAG laser at 1064 nm. The pulse repetition rate is 80 Hz, pulse energy is 0.7 mJ and the full width at half maximum (FWHM) pulse width is 4 ns. The beam divergence angle is about 2 mrad. Silicon avalanche photodetector (APD) is used in the receiver. Data sampling is achieved using LeCroy 6880B A/D converter at 1.35 gagesample per second (GS/s). The platform is a Sabreliner T-39. At an operation altitude of 5,000 m above the ground, the laser footprint has a diameter of about 10 m.

VCL: The Vegetation Canopy Lidar (VCL) is the first selected mission of NASA's new Earth System Science Pathfinder (ESSP) program. The VCL mission was proposed by the University of Maryland, NASA GSFC, and other universities and industrial collaborators. The principal goal of VCL is to characterize the three-dimensional structure of the earth, in particular, canopy vertical and horizontal structure and land surface topography. It is a satellite-borne lidar system, and is proposed to launch soon [34]. The VCL is a so-called Multi-Beam Laser Altimeter (MBLA) and adopts three Q-switched Nd:YAG lasers at 1064-nm with a pulse repetition rate of 290 Hz, and a laser pulse energy of 10 mJ. The orbital altitude is 400-km with an inclination angle of 65°, which provide near-complete coverage of vegetation areas of interests. The beam spacing is 4 km in a circular configuration. The detector FOV is as large as 25 m. A 0.9-m diameter beryllium telescope is adopted as the optical receiver. Silicon APD detectors are used in the telescope focal plane and the data sampling rate is 250 MS/s.

Commercial airborne vegetation lidar systems are difficult to find in the market. During recent years, commercial small footprint laser altimeters were used in some airborne vegetation applications. The Airborne Laser Terrain Mappers (ALTM) system manufactured by Optech in Canada, although not specifically designed for vegetation application, has been used in several vegetation surveys [27], [35]. The ALTM typically adopts solid state laser at near infrared, the PRF can be as high as 50 kHz, and the range accuracy is several centimeters. It is a compact system that has been packed to fly aboard various aircrafts.

1.3 Lidar Vegetation Remote Sensing

There is a great demand for vegetation remote sensing. Traditional on-site vegetation characterization is time consuming and it is difficult to obtain data from remote areas. Even worse, for some places like the tropical forests, even if the researchers can gain access, accurate data are still hard to measure when the trees are dense and tall [36]. The emergence of lidar provides a new tool for vegetation remote sensing. Because of the characteristics of the laser beam, lidars are able to provide information on vegetation height, vegetation structure, vegetation topography, vegetation tomography, and vegetation dynamics. It is expected to make global vegetation remote sensing faster and more accurate. During recent years, there has developed a growing interest in the applications of lidar towards vegetation remote sensing. One of the most important features of lidar vegetation remote sensing is the ability to detect the vegetation canopy structure.

1.3.1 Importance of Vegetation Canopy Remote Sensing

The vegetation canopy is composed of leaves, trunk, twigs, branches and other phytoclements. As is well known, the vegetation canopy is a very important element of the ecosystem. The canopy structure refers to the qualitative and quantitative composition of the vegetation and the spatial arrangements of these elements [36]. The vegetation canopy structure has a great impact on the interaction between the vegetation and the physical environment. For example, the surface energy exchange, the mass and heat transportation, the transpiration, photosynthesis and other biophysical and biochemical mechanisms are all functioned through the vegetation canopy. Appropriately planned canopy structure will enable the vegetation to make efficient use of the solar radiation energy [37]. The study of the vegetation canopy is also very helpful to the understanding of the microclimate generated by the vegetation. The sophistication of the vegetation microclimate models requires detailed descriptions of the canopy geometrical

structures [38]. These models are very important since the microclimate may have an impact on a much larger scale climate change. Canopy structure is also correlated to many ecological questions. Therefore, a good understanding of the canopy structure will contribute to the management of a sustainable ecosystem.

One especially important area of vegetation remote sensing is forest remote sensing. Lidar is used to directly measure the forest canopy height, canopy vertical distribution (including sub-canopy structure); and can also be applied to estimate stand volume, basal area, mean stem diameter and above ground biomass, etc [10]-[30]. These forest parameters are useful for the identification, characterization and protection of the forest, and will support a sustainable forest management plan to protect the forest from stress conditions or excessive logging.

1.3.2 Advantages of Vegetation Lidar

One advantage of a lidar system over other remote sensing tools is the ability to acquire the vertical structure of vegetation canopy, which is especially important for forest remote sensing. Lidar is used for vegetation canopy structure and sub-canopy structure measurement. Laser beam can penetrate into the gaps of the canopy and the backscattered radiation from the phytoelements in the vegetation stand is recorded as a function of height from the canopy top to the ground. The recorded lidar waveform provides useful information about canopy and sub-canopy structures. Generally speaking, passive remote sensing techniques do not have the ability to acquire the vegetation canopy structure. While the synthetic aperture radar (SAR) has certain ability, it is limited by its wavelength, therefore, unable to obtain the vegetation sub-canopy structure. On the other hand, a lidar has a better spatial resolution which is high enough to detect the sub-canopy structure, because of the shorter wavelength. If the vertical and horizontal structure data of the vegetation are combined together, they will lead to the vegetation tomography which can fully describe the vegetation in three dimensions.

Previous research also demonstrated that the radar signal tends to saturate when vegetation becomes dense. The research showed that the criterion for saturation is 100 Mg/ha at P-band, 40 Mg/ha at L-band, and 20 Mg/ha at C-band [39]. Other studies also confirmed that a SAR is insensitive to differences in forest biomass above 150 Mg/ha [40], which is well below values for many tropical or even temperate forests. This imposes a great limitation on above ground biomass estimation using a SAR for a dense forest. It was discovered, however, that lidar could work in a much denser vegetation condition without signal saturation, and was capable of determining the above ground biomass [12], [13], [22], [24], [26]. For example, lidar is able to predict the above ground biomass nonasymptotically to 450 Mg/ha in the Douglas-fir [12] and Western Hemlock forests [26] with high accuracy. Effort was also made on using lidar to estimate the structure and biomass of a neotropical rainforest [29].

Study also demonstrated that although Interferometric SAR (INSAR) could be used to retrieve the Digital Elevation Map (DEM) and the vegetation height, the performance of obtaining true ground DEM degraded over vegetated area. However, by taking use of the lidar scanning data, the accuracy of DEM and vegetation height measurements were improved [35].

Lidar provides a unique tool for vegetation remote sensing, especially when vertical canopy structure is involved. Since it is still a relatively new technology, more applications of lidar in vegetation remote sensing need to be explored.

1.3.3 Vegetation Vertical Structure Detection

Previous applications involved the use of laser altimeters, which are designed for measuring the range between the altimeter and the strongest laser return. Some recent altimeters also implemented the ability to digitize and record part of the return laser energy, which makes it possible to acquire the vegetation vertical canopy structure through the laser altimeters. This has great advantage over passive optical remote sensing, which do not have the ability to acquire

canopy vertical distribution. Using a laser altimeter, a true ground DEM can be obtained by removing the vegetation cover from the recorded data during data processing.

Early laser altimeters typically have small footprint (less than 1 m), range-only detection and work at low altitude. It was revealed that a small footprint lidar may frequently miss the canopy tops, therefore, lead to underestimation of the canopy height [14]. Another problem with small footprint lidar is that for a particular laser shot, it is very difficult to determine whether that shot really penetrated through the canopy to the ground [16], [20], [22], [26]. However, study by a Finland group showed that using high PRF and small footprint laser scanner, it is possible to locate each individual tree and estimate single stand forest attributes [21]. However, with high PRF lidar, it is impractical to digitize the entire lidar waveform, due to the limitations of data sampling rate, data transfer rate and data storage capacity. Such a system usually samples only the first and the last return of the laser shot. In addition, this approach is only applicable to small-scale remote sensing applications. For regional or global applications, the data stream will be overwhelmingly large. Therefore, it would be technologically challenging and cost inefficient to use such a small footprint laser scanner in large-scale applications.

With the recent technology development, new lidar systems with full waveform sampling ability and larger footprint were developed. Using a large footprint lidar such as SLICER, the canopy height, above ground biomass, basal area and other stand attributes can be obtained. Through the lidar waveform, an integrated canopy structure/substructure distribution is also obtained. The proposed satellite borne lidar system VCL will sample the Earth's closed canopy forests and characterize the three-dimensional structure of the Earth surface on a global scale. It will provide improved forest canopy height estimation, which will lead to better biomass estimation. VCL provides a new tool to characterize, monitor and predict the land cover for the terrestrial ecosystem modeling, the global forest dynamics, the global carbon-cycle modeling and the global climate modeling.

1.3.4 Lidar Polarimetric Measurement

Most vegetation remote sensing lidars are not polarimetric systems. However, the ability to study the polarimetric properties of vegetation is of great importance. It is technically more difficult to implement polarimetric ability to a lidar system than to a radar. The ALPS system is among the few sensors that have the polarimetric measurement ability. Although it has enough receiving channels to characterize the full polarization state of the backscattered laser beam, field studies of vegetation showed that the signal to noise ratio (SNR) for the circular polarization channel was too low. Usually only the co-polarized and cross-polarized channels were used. The ALPS system was applied to forest ecosystems dynamics experiments [41]. Using ALPS system, distinct depolarization signatures for different tree species were observed. For example, the study demonstrated that the depolarization increase was significantly correlated with the increase of leaf roughness for the broadleaf trees at near infrared. However, this was not observed for coniferous trees, which had lower average depolarization values. Also, coniferous trees showed distinct depolarization signatures at green wavelength [42]. The research also revealed that near infrared depolarization was strongly correlated with crop parameters such as the nitrogen fertilization; and the depolarization spectral difference index could be used for yield estimation [43]. Unfortunately, the ALPS system did not acquire the lidar waveform, and thus was unable to obtain the vegetation vertical structure.

1.4 Motivation for a New Lidar Sensor

To support its Airborne Remote Sensing Program, the University of Nebraska decided to develop an airborne lidar sensor. Requirements of the sensor included multiwavelength detection, polarimetric detection and lidar waveform acquisition. A flying altitude of more than 1 000 m above the ground and a medium laser footprint also needed to be satisfied. To meet the above requirements, a Multiwavelength Airborne Polarimetric Lidar (MAPL) system has been designed

and developed [44]. This system employs a Nd:YAG laser which emits radiation at two wavelengths: the fundamental at 1064 nm and the frequency-doubled at 532 nm. Both laser beams are highly linearly polarized (100: 1 distinction ratio) and have a beam divergence angle of ~ 4 mrad. The receiver consists of four channels, which enable dual-wavelength and dual-polarization detection. The two polarization directions are co-polarization and cross-polarization. In addition to the polarimetric information that can be gathered, the MAPL system also has ranging capability and is able to digitize and record the entire lidar waveform. Thus, it is capable of performing studies of vegetation canopy structure as well as characterization of vegetation depolarization. The system has been packaged to fly aboard a Piper Saratoga aircraft from a typical altitude of 2000 m above the ground.

1.5 Organizational Overview

This dissertation is organized as follows. In Chapter 2, the MAPL system components are described in detail. Chapter 3 deals with theoretical aspects of the remote sensing lidar. A general form of lidar range equation is developed, and the theory and application considerations are briefly discussed. Signal to noise ratio (SNR) considerations are investigated in Chapter 3. The vegetation vertical distribution model is discussed in Chapter 4. Both single tree and forest 3-D models are developed, which can be used for the modeling of the vegetation lidar waveform. Chapter 5 describes the optical alignment of the MAPL system. Chapter 6 provides the results of polarimetric calibration efforts. Stokes parameters of various materials, which are targeted for applications as polarimetric calibration standards, were measured in the laboratory. The range measurement ability is discussed in Chapter 7. The range measurement is field tested and calibrated. Extended tests on vegetation applications are presented in Chapter 8, to validate the capability of the MAPL system in vegetation remote sensing. Finally, Chapter 9 provides conclusions and future research directions.